Civil and Environmental Engineering

College of Engineering and Computer Science

# Soil Mercury and its Response to atmospheric Mercury Deposition across the Northeastern United States

Xue Yu
*Syracuse University*

Charles T. Driscoll
*Syracuse University*

Richard A. F. Warby
*Assumption College*

Mario Montesdeoca
*Syracuse University*

Chris E. Johnson
*cejohns@syr.edu*

Follow this and additional works at: https://surface.syr.edu/cie

Part of the Civil and Environmental Engineering Commons

### Recommended Citation

# Soil mercury and its response to atmospheric mercury deposition across the northeastern United States

Xue Yu,[1,3] Charles T. Driscoll,[1] Richard A. F. Warby,[2] Mario Montesdeoca,[1] and Chris E. Johnson[1]

[1]*Department of Civil and Environmental Engineering, Syracuse University, Syracuse, New York 13244 USA*
[2]*Department of Natural Sciences, Assumption College, Worcester, Massachusetts 01609 USA*

*Abstract.* Terrestrial soil is a large reservoir of atmospherically deposited mercury (Hg). However, few studies have evaluated the accumulation of Hg in terrestrial ecosystems in the northeastern United States, a region which is sensitive to atmospheric Hg deposition. We characterized Hg and organic matter in soil profiles from 139 sampling sites for five subregions across the northeastern United States and estimated atmospheric Hg deposition to these sites by combining numerical modeling with experimental data from the literature. We did not observe any significant relationships between current net atmospheric Hg deposition and soil Hg concentrations or pools, even though soils are a net sink for Hg inputs. Soil Hg appears to be preserved relative to organic carbon (OC) and/or nitrogen (N) in the soil matrix, as a significant negative relationship was observed between the ratios of Hg/OC and OC/N ($r$ = 0.54, $P$ < 0.0001) that shapes the horizonal distribution patterns. We estimated that atmospheric Hg deposition since 1850 (3.97 mg/m$^2$) accounts for 102% of the Hg pool in the organic horizons (3.88 mg/m$^2$) and 19% of the total soil Hg pool (21.32 mg/m$^2$), except for the southern New England (SNE) subregion. The mean residence time for soil Hg was estimated to be 1800 years, except SNE which was 800 years. These patterns suggest that in addition to atmospheric deposition, the accumulation of soil Hg is linked to the mineral diagenetic and soil development processes in the region.

*Key words: atmospheric mercury deposition; mercury; soil carbon; soil profile; spatial pattern.*

## Introduction

Mercury (Hg) is a toxic metal that biomagnifies as methyl Hg through food chains, resulting in exposure and potential health effects both to wildlife and humans (Driscoll et al. 2007, 2013). Atmospheric deposition is the main source of Hg to remote environments (Fitzgerald et al. 1998), and soils are the major receptor of atmospheric Hg deposition in terrestrial ecosystems (Grigal 2002), as well as a substantial contributor of Hg to most surface waters (Swain et al. 1992, Hurley et al. 1995, Selvendiran et al. 2008). Studies have shown terrestrial biota (e.g., salamanders, birds, bats) with elevated Hg concentrations (Evers et al. 2007, 2008, 2012, Rimmer et al. 2010, Townsend and Driscoll 2013). Hence, quantifying the pools and dynamics of Hg in soils is of vital importance in understanding the biogeochemistry and global cycling of this element.

Natural sources and cycling (volcanoes, geological diagenesis, surface evasion, and biomass burning; 5207 Mg/yr) contribute more Hg emissions than primary anthropogenic sources (coal-fired power plants, municipal waste incinerators, industrial processes; 2320 Mg/yr;

Pirrone et al. 2010). Even though primary anthropogenic sources are only about one-third of the total annual emissions to the atmosphere, anthropogenic Hg emissions are at least an order of magnitude greater than geogenic sources, due to the reemission of previously deposited Hg (secondary sources, Driscoll et al. 2013). The transport of Hg from the atmosphere to the land surface is mainly through wet and dry deposition. In forest ecosystems, overstory canopies substantially enhance atmospheric Hg deposition via litterfall and throughfall deposition (St. Louis et al. 2001, Demers et al. 2007, Risch et al. 2011). Elemental Hg (Hg$^0$) can be volatilized from land and water into the atmosphere, thus the transfer of Hg between the atmosphere and Earth surfaces is bidirectional (Denkenberger et al. 2011).

In surface soils, Hg is supplied in litter inputs and precipitation/throughfall Hg inputs that are adsorbed to soil organic matter (SOM). Conceptually, soil Hg is processed in cohorts of SOM whose lability decrease and Hg residence time increases with age (Smith-Downey et al. 2010). Mercury can be reduced in surface soils through the oxidation of SOM and evaded back to the atmosphere (Smith-Downey et al. 2010). The major form of Hg in surface soils is ionic Hg that is bound to humic substances in soil organic matter (Grigal 2002). Past atmospheric Hg deposition is largely associated with recalcitrant SOM and is referred to as legacy Hg,

FIG. 1. Locations of the soil sampling sites across the northeastern United States, which are divided into five subregions by geographic proximity: Adirondacks (ADR), Catskills/Poconos (CATPOC), Central New England (CNE), Maine, and Southern New England (SNE).
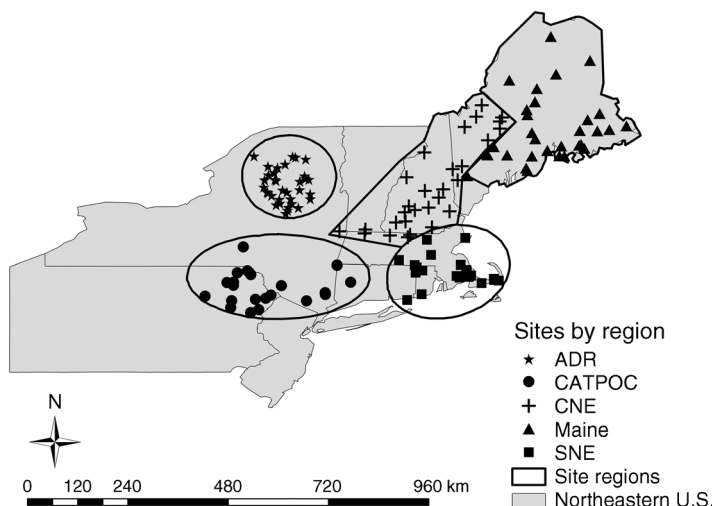
which has a long residence time in soil (Hintelmann et al. 2002, Dittman et al. 2010). The horizonal patterns (i.e., spatial configuration) of soil Hg concentrations may not be directly related to current atmospheric Hg deposition due to accumulation of legacy Hg, differential inputs, accumulation and losses of SOM, and the transport and dynamics of both Hg and SOM (Obrist et al. 2011). Hence, due to the important regulating effect in Hg transport, SOM concentrations are often used to estimate the distribution of soil Hg concentrations (Smith-Downey et al. 2010).

Mercury contamination is a significant issue in the northeastern United States due to its toxicity and elevated concentrations of methyl Hg in fish and wildlife (Evers et al. 2007). We surveyed soil Hg concentrations across the northeastern United States, providing the most comprehensive survey of soil Hg concentrations for this region. Based on the survey, we examined concentrations and pools of Hg in organic and mineral soils, their relation to SOM, soil development, and estimated net atmospheric Hg deposition to land surfaces in each of the subregions of the Northeast. We examined the following hypotheses: (1) terrestrial soils in the northeastern United States are a net sink for Hg inputs (i.e., atmospheric deposition inputs are greater than soil surface $Hg^0$ evasion), (2) concentrations and pools of soil Hg are positively correlated with current net deposition of Hg, and (3) soil organic carbon (OC) and nitrogen (N) are important regulators (i.e., controller) of the horizonal patterns and pools of soil Hg.

## METHODS

### Study sites

During the summers of 2001 and 2002, we collected soils from 139 sites within the watersheds of the Direct/Delayed Response Program (DDRP; Fig. 1), which was initially designed to quantify the acid-base chemistry of surface waters in the northeastern United States (Lee et al. 1989). The DDRP study watersheds have been well characterized for landscape and soil physicochemical properties (Church et al. 1989, Warby et al. 2005, 2009). The sampling sites are clustered into five subregions according to geographic proximity: Adirondacks (ADR), Catskills/Poconos (CATPOC), Central New England (CNE), Maine, and Southern New England (SNE). The number of sites sampled and the biophysical characteristics of the subregions are summarized in Table 1. The study region is largely covered by forests (Table 1a; U.S. Geological Survey, 2011), with the major deciduous forest classes of maple–beech–birch (26.7%) and oak–hickory (22.9%), coniferous forest of white, red, and jack pine (13.9%) and spruce–fir (11.8%), and mixed forest of oak–pine (3.6%).

### Soil sample collection and analysis

One soil pit was excavated in each of the DDRP watersheds. We designated soil horizons following U.S. Soil Survey conventions (Arnold and Eswaran 1993), where four master horizons were used, i.e., O, E, B, and C horizons. O horizons are layers dominated by organic materials, which include the slightly decomposed (Oi), moderately decomposed (Oe), and highly decomposed (Oa) horizons. We grouped the Oi and Oe horizons as a single Oie horizon for sampling purposes. The E horizon is the mineral horizon often found below the O horizons, characterized by the eluviation of silicate clay, iron, aluminum, or a combination of these. The B horizons, which were broadly delineated as $B_{S1}$, $B_{S2}$, and $B_{S3}$ in this study, are layers which may contain concentrations of clay or organic material due to illuviation. The C horizons are layers that are little affected by soil forming processes, often glacial till in the northeastern United States. From each excavated pit, samples were collected from these seven horizons, if present, with the number of horizons sampled in each subregion shown in Table 1b. Soil horizons were determined using soil color, structure, and C contents (Warby et al. 2009, Golden 2010).

TABLE 1.  Characteristics of the subregions and site sampling information.

| | | a) Characteristics of the subregions | | | | | b) Number of soil samples excavated in each soil horizon | | | | | | | |
| Subregion | pH | Precipitation (mm) | Area ($10^6$ ha) | Elev (m) | Forest cover (%) | Temp, °C min–max | Oie | Oa | E | $B_{S1}$ | $B_{S2}$ | $B_{S3}$ | C | Total pits |
|---|---|---|---|---|---|---|---|---|---|---|---|---|---|---|
| ADR | 3.9 | 1290 | 2.5 | 560 | 96 | −0.8–11.3 | 31 | 23 | 23 | 27 | 27 | 20 | 19 | 34 |
| CATPOC | 3.8 | 1300 | 5.2 | 410 | 79 | 2.3–13.9 | 17 | 13 | 6 | 18 | 18 | 12 | 8 | 21 |
| CNE | 3.7 | 1300 | 4.8 | 270 | 91 | −0.3–11.6 | 34 | 21 | 18 | 31 | 32 | 26 | 20 | 34 |
| Maine | 3.3 | 1270 | 6.6 | 150 | 90 | −1.0–10.5 | 20 | 0 | 14 | 23 | 19 | 13 | 5 | 27 |
| SNE | 3.6 | 1310 | 2.0 | 60 | 76 | 4.4–14.9 | 18 | 8 | 7 | 20 | 20 | 14 | 3 | 23 |

*Notes:* The pH is referring to pH of the extract soil sample solution, where mean values of the soil samples in each subregion were reported here. Forest cover refers to the percent forest cover in each watershed where soil samples were excavated. Subregion abbreviations are Adirondacks (ADR), Catskills/Poconos (CATPOC), Central New England (CNE), Maine, and Southern New England (SNE).

In each pit, samples were collected from all horizons greater than 3 cm in thickness down to the bedrock or to 1.5 m. After collection, all the soil samples were air dried, double bagged, stored in plastic freezer bags, and then sent to Syracuse University for analysis. For further details regarding the criteria for soil pit location and method of excavation, refer to Warby et al. (2009).

We determined total Hg concentrations for all horizons using a Milestone DMA-80 Direct Mercury Analyzer (Milestone, Microwave Laboratory Systems, Shelton, Connecticut, USA), thermal decomposition, amalgamation/atomic absorption spectrophotometer (TDA/AAS) based on U.S. Environmental Protection Agency (EPA) Method 7473. We measured total organic carbon content (OC) and total nitrogen content (N) on samples from all horizons and total sulfur content (S) on samples from organic horizons, using a Costech ECS 4010 CHNSO analyzer (Costech Analytical Technologies, Valencia, California, USA). Quality assurance and quality control procedures (QA/QC) for all chemical analyses can be found in Appendix A.

The statistical analyses were carried out using the Statistic Analysis System (SAS 9.2; SAS Institute, Cary, North Carolina, USA) software. We analyzed correlations using SAS PROC CORR. We used Tukey's multiple comparisons method to compare variables in different soil horizons and Principle Component Analysis and PROC GLM to analyze parameters affecting soil Hg concentrations and pools.

### Estimation of current Hg deposition

Total atmospheric Hg deposition was estimated as the sum of wet and dry deposition. Wet Hg deposition was calculated as the product of annual volume-weighted precipitation Hg concentrations (data obtained from the National Atmospheric Deposition Program Mercury Deposition Network; NADP MDN 2011) and the quantity of annual precipitation (data obtained from PRISM, Parameter-elevation Regressions on Independent Slopes Model [Daly et al. 1997]). We divided the northeastern United States into forested and nonforested land areas and estimated dry atmospheric Hg deposition to these areas separately. In nonforested areas, dry deposition was estimated as the deposition of gaseous oxidized Hg plus particulate bound Hg obtained from CAMQ-Hg output (U.S. EPA, Community Multiscale Air Quality [CMAQ 2005]). In the forested areas, dry deposition was estimated as the net throughfall Hg (throughfall Hg minus wet Hg deposition) and litterfall Hg deposition (pathway of $Hg^0$ deposition). The net atmospheric Hg flux was calculated as the estimated atmospheric Hg deposition minus surface $Hg^0$ evasion. The details of the application of this method to estimate atmospheric Hg deposition involving litterfall and throughfall Hg deposition and $Hg^0$ evasion are provided in Appendix A and in Yu et al. (2013).

Our estimates suggest that the fluxes of dry Hg deposition (mean, 16.7 $\mu g \cdot m^{-2} \cdot yr^{-1}$; range, 1.9–68.7 $\mu g \cdot m^{-2} \cdot yr^{-1}$) were greater than wet Hg deposition (9.8 $\mu g \cdot m^{-2} \cdot yr^{-1}$; 3.5–19.2 $\mu g \cdot m^{-2} \cdot yr^{-1}$) in 92% of the total area of the northeastern United States that includes the DDRP subregions (Fig. 2). Both dry and wet deposition were highest in the CATPOC and the ADR subregions ($P < 0.0001$), and values decreased with increasing latitude and decreasing longitude. All five subregions showed positive net atmospheric Hg deposition (i.e., atmospheric deposition exceeded evasion). The mean ratios of net total Hg deposition to wet Hg deposition and the current net total atmospheric Hg deposition are presented in Table 2. The total atmospheric Hg deposition to the land area of five subregions in the northeastern United States (21 million ha) was estimated to be 4530 kg/yr (mean flux, 21.93 $\mu g \cdot m^{-2} \cdot yr^{-1}$; wet deposition, 1440 kg/yr; dry deposition, 3090 kg/yr), while total $Hg^0$ evasion was estimated as 1740 kg/yr (8.20 $\mu g \cdot m^{-2} \cdot yr^{-1}$).

### Reconstruction of historical Hg deposition

It is suggested that anthropogenic Hg emissions before 1850 account for 40% of the total cumulative human emissions (Streets et al. 2011). To calculate cumulative Hg load from the atmosphere since 1850, we assumed Hg deposition to be constant before 1850. Using the ratio of total Hg deposition/wet Hg deposition modeled in this study (mean value, 1.94) and the preindustrial (1850) Hg wet deposition of 3 $\mu g \cdot m^{-2} \cdot yr^{-1}$ both estimated by Lorey and Driscoll (1999) for Little Echo Pond in the Adirondacks (a perched seepage lake)
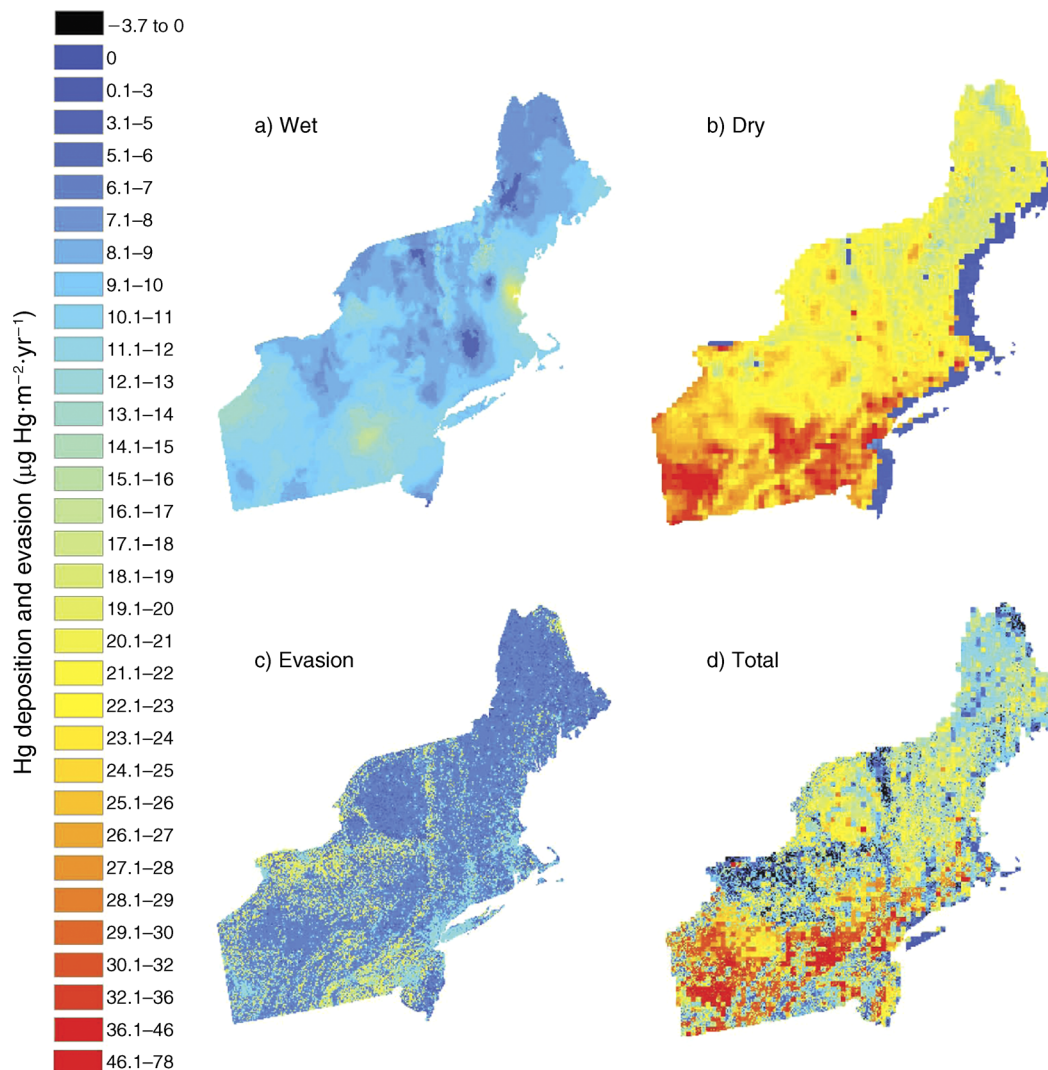
Fig. 2.   Estimated atmospheric Hg deposition and surface elemental $Hg^0$ evasion in the northeastern United States. Plots show (a) wet Hg deposition and (b) dry deposition. Dry deposition was estimated as dry deposition of oxidized Hg (gaseous $Hg^{2+}$ and particulate bound Hg) obtained from CAMQ-Hg output (U.S. EPA, Community Multiscale Air Quality) in the nonforested areas and net throughfall deposition (throughfall deposition minus wet deposition) and litterfall deposition (pathway of $Hg^0$) in the forested areas. Plots show (d) total net Hg deposition which was estimated as (c) the sum of wet and dry deposition minus $Hg^0$ evasion.

and Bookman et al. (2008) for Glacial Lake in central New York State (a glacial plunge pool), we estimated the flux of preindustrial Hg deposition (e.g., 9.35 $\mu g \cdot m^{-2} \cdot yr^{-1}$ for the northeastern United States). The historical record obtained from paleolimnological studies suggests that atmospheric Hg deposition has increased steadily (two- to three-fold) since the onset of industrialization until the late 1900s (Swain et al. 1992, Fitzgerald et al. 1998, Lorey and Driscoll 1999, Schuster et al. 2002, Biester et al. 2007). Studies have also indicated that regional Hg deposition has decreased in recent decades, which is coincident with efforts to control Hg emissions in North America (Engstrom and Swain 1997, Driscoll et al. 2007, Drevnick et al. 2011, Schmeltz et al. 2011). Studies suggest that Hg deposition

TABLE 2.   Estimated historical total Hg deposition to subregions in the northeastern United States, while the deposition after 1850 was reconstructed from previous studies on Hg emissions. Subregion abbreviations defined in Table 1.

| | Deposition | | | |
|---|---|---|---|---|
| Subregion | Dry : wet | Current total ($\mu g \cdot m^{-2} \cdot yr^{-1}$) | Pre-1850 ($\mu g \cdot m^{-2} \cdot yr^{-1}$) | Load after 1850 ($mg/m^2$) |
| ADR | 2.31 | 23.79 | 9.93 | 4.29 |
| CATPOC | 2.47 | 26.54 | 10.42 | 4.73 |
| CNE | 2.05 | 21.52 | 9.16 | 3.89 |
| Maine | 2.21 | 17.10 | 9.62 | 3.21 |
| SNE | 1.54 | 20.69 | 7.62 | 3.72 |
| Average | 2.12 | 21.93 | 9.35 | 3.97 |

Notes: The deposition before industrialization (<1850) was considered to be steadfast at each of the subregions. See Fig. 3 for a graph of reconstruction of Hg deposition after 1850.
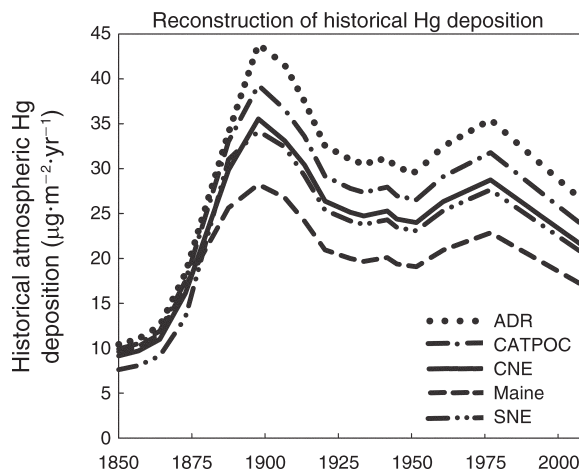
FIG. 3. Reconstruction of Hg deposition after 1850 from previous studies on Hg emissions. Subregion abbreviations defined in Fig. 1. See Table 2 for atmospheric Hg deposition data.

peaked around the 1890s due to mining, and again in the 1970s largely due to coal combustion (Streets et al. 2011, Amos et al. 2013), then declined recently (a 25% decrease rate from the 1970s to current flux suggested by Driscoll et al. 2007 and Drevnick et al. 2011). Hence, we reconstructed historical total Hg deposition in each subregion (Fig. 3). Note that this calculation assumes that land cover remains constant historically from current conditions. This is obviously a poor assumption as there have been marked changes in land cover in the northeastern United States over the past 150 years or so (e.g., Driscoll et al. 2003). Unfortunately we do not have historical land cover information for these regional sites, so this assumption is an important limitation to this calculation. The sum of annual total Hg for the period 1850 to present (time of soil sampling) represents the cumulative Hg load from the atmosphere.

### Soil Hg pool estimation

Estimating the pool of Hg in terrestrial soils is important to quantify Hg cycling and fate in the environment. However, the natural complexity of soil (Howard and Howard 1989) and the variations of Hg concentrations in soil profiles make it difficult to quantify the mass of Hg in soils. We thought it more meaningful to calculate the Hg pool by subtracting the background soil Hg concentrations in order to examine Hg accumulation in soils. Hence, Hg in the E and C horizons was not included to the total soil Hg pool. The concentrations of Hg in coarse fragments (>2 mm) were also considered to be the background Hg concentrations, although this may underestimate the Hg pool in the organic horizons. Hence, the soil Hg pool was estimated as the product of soil Hg concentrations (with the background Hg concentration subtracted) and the fine soil mass (<2 mm), while the soil mass was calculated as the product of horizon thickness and soil

bulk density (Huntington et al. 1989, Federer et al. 1992, De Vos et al. 2005). We used the relationships developed by Huntington et al. (1989) to calculate soil Hg pool, which was a study in New Hampshire and covered soils down to the C horizon (OC > 5 mg/g). The functions are

$$P_i = (C_i - C_b) \times B_i \times T_i \times (1 - F_i) \qquad (1)$$

$$\ln(B_i) = 0.263 - 0.147\ln(\text{OC‰})_i - 0.103\ln(\text{OC‰})_{i2} \quad (2)$$

where $P_i$ is the soil Hg pool (mg/m$^2$), $C_i$ is the soil Hg concentration (ng/g), $C_b$ is the background soil Hg concentration (see *Results: Correlation analysis*), $B_i$ is the bulk density of the fine earth (<2 mm; Mg/m$^3$), $T_i$ is the horizon thickness (cm), $F_i$ is the fraction of coarse fragment by volume (%), OC is the soil organic carbon concentration (mg/g), and $i$ is the specific horizon.

### RESULTS

#### Soil Hg concentrations and pools

Soil Hg concentrations varied considerably from site to site. Soil Hg concentrations in the organic horizons in the ADR and CATPOC subregions were found to be significantly higher than in the other subregions ($P = 0.002$; Table 3a). Mercury concentrations decreased with increasing soil depth, with higher concentrations in the organic horizons and lower concentrations in the mineral horizons (Table 3a). Mercury concentrations were higher and more variable in the organic horizons than in the mineral horizons. Among the 65 sites across the five subregions where both organic horizons were sampled, 39 of the sampling sites (61%) had greater Hg concentrations in the Oa than in the Oie horizons. Contrary to other subregions, Hg concentrations in the Oie horizons were greater than in the Oa horizons at all five sampling sites in the SNE subregion where both horizons were sampled.

The soil types in the study region of the northeastern United States are varied, but are generally derived from glacial till. Both organic horizons (Oie and Oa) were acidic, with average pH values (pH$_S$) of 3.7 in the Oie and 3.2 in the Oa horizon (Table 1a). Soils in SNE had lower concentrations of organic carbon (OC), as they were sandy compared to soils in other subregions (Table 3b). Both OC and N concentrations decreased with increasing soil depth. In general, soil OC mass concentrations were approximately 20 times greater than N concentrations in each horizon. The average sulfur (S) concentrations in the Oie and Oa horizons were 1.8 ± 1.2 mg/g and 1.1 ± 0.6 mg/g, respectively. Concentrations of soil OC, N, and S were significantly correlated (OC vs. N, $r = 0.97$; OC vs. S, $r = 0.77$; and N vs. S, $r = 0.81$; all $P$ values are <0.0001), suggesting that S in the soils is primarily organic.

The thicknesses of the soil horizons differed among various sites, with shallower organic horizons in SNE than the other subregions (Table 3c). The fraction of coarse fragments ranged from 2–5% in the organic

TABLE 3. General statistics (mean ± SD) of soil Hg concentrations and pools and physical chemical characteristics (carbon concentrations, thickness, and bulk density) in the five subregions.

| Subregion | Oie | Oa | $B_{S1}$ | $B_{S2}$ | $B_{S3}$ |
|---|---|---|---|---|---|
| a) Hg concentrations (ng Hg/g soil) | | | | | |
| ADR | 196.4 ± 47.2 | 238.6 ± 99.0 | 102.1 ± 37.4 | 77.9 ± 31.6 | 46.3 ± 28.4 |
| CATPOC | 235.3 ± 54.1 | 272.9 ± 114.2 | 80.2 ± 42.7 | 67.7 ± 56.8 | 34.6 ± 15.6 |
| CNE | 167.0 ± 58.5 | 191.6 ± 77.8 | 83.8 ± 40.7 | 70.2 ± 39.5 | 51.9 ± 24.2 |
| Maine | 150.8 ± 74.9 | ND | 96.6 ± 47.2 | 71.8 ± 27.3 | 61.9 ± 44.3 |
| SNE | 164.4 ± 67.0 | 131.8 ± 37.9 | 34.2 ± 15.7 | 31.9 ± 15.0 | 17.3 ± 11.3 |
| b) Carbon concentrations (mg C/g soil) | | | | | |
| ADR | 321 ± 136 | 453 ± 86 | 56 ± 18 | 35 ± 17 | 22 ± 16 |
| CATPOC | 251 ± 123 | 418 ± 82 | 25 ± 10 | 14 ± 13 | 4 ± 5 |
| CNE | 227 ± 123 | 369 ± 133 | 34 ± 19 | 18 ± 14 | 13 ± 12 |
| Maine | 276 ± 135 | 406 ± 114 | 40 ± 22 | 17 ± 9 | 12 ± 18 |
| SNE | 253 ± 3 | 337 ± 117 | 16 ± 9 | 8 ± 5 | 2 ± 2 |
| c) Thickness (cm) | | | | | |
| ADR | 4.9 ± 1.5 | 4.4 ± 2.3 | 12.2 ± 5.4 | 21.0 ± 9.6 | 20.9 ± 15.7 |
| CATPOC | 4.1 ± 1.5 | 2.8 ± 1.4 | 16.7 ± 9.2 | 18.5 ± 10.6 | 28.1 ± 12.4 |
| CNE | 4.8 ± 1.7 | 3.8 ± 3.2 | 11.7 ± 6.4 | 22.1 ± 9.9 | 25.2 ± 11.8 |
| Maine | 6.4 ± 2.8 | 1.7 ± 1.6 | 13.5 ± 10.5 | 17.9 ± 8.1 | 32.3 ± 20.2 |
| SNE | 5.5 ± 2.8 | 2.0 ± 1.4 | 12.5 ± 7.7 | 26.8 ± 16.7 | 20.9 ± 11.9 |
| d) Bulk density ($Mg/m^3$) | | | | | |
| ADR | 0.17 ± 0.05 | 0.27 ± 0.14 | 0.68 ± 0.05 | 0.69 ± 0.06 | 0.72 ± 0.09 |
| CATPOC | 0.18 ± 0.04 | 0.32 ± 0.13 | ND | ND | ND |
| CNE | 0.24 ± 0.15 | 0.36 ± 0.17 | 0.69 ± 0.07 | 0.77 ± 0.02 | ND |
| Maine | 0.21 ± 0.21 | 0.29 ± 0.12 | 0.65 ± 0.10 | ND | ND |
| SNE | 0.24 ± 0.24 | 0.47 ± 0.21 | ND | ND | ND |

*Notes:* ND means no data. Subregion abbreviations defined in Table 1.

horizons and around 20% in the mineral horizons, and they were much higher in CATPOC subregion (organic horizon, 13%; mineral, 27% in average). The bulk densities were lower in the organic horizons than in the mineral horizons (Table 3d). The total pool of soil Hg showed no significant differences among the subregions with an average value of 21.32 mg/m$^2$, with the exception of SNE, which was substantially lower than the other subregions (9.62 mg/m$^2$; Table 4). Note that the estimation of Hg pool in the mineral horizons in SNE is somewhat uncertain due to the limited number of observations for this subregion. The fraction of the total Hg pool occurring in the organic horizons had a mean of 21% and ranged from 12% (Maine) to 33% (SNE).

### Correlation analysis

In surface organic soils, we found strong correlations between Hg concentrations and S concentrations in both Oie ($r = 0.55$, $P < 0.0001$) and Oa ($r = 0.69$, $P < 0.0001$) horizons. We found Hg concentrations were correlated with soil OC and N concentrations in all horizons. The relationships were more significant in the mineral horizons (Hg vs. OC, $r = 0.73$; Hg vs. N, $r = 0.70$) than in the organic horizons (Hg vs. OC, $r = 0.37$; Hg vs. N, $r = 0.42$; all $P$ values $< 0.0001$). The relationship of soil Hg concentrations with SOM has been used to estimate background or native soil Hg concentrations (Hissler and Probst 2006). We estimated the background soil Hg concentration as the intercept of the relationship between soil Hg concentrations and OC concentrations. The background Hg concentration estimated for the five subregions across the northeastern United States was 20.0 ng/g (Fig. 4a).

We also examined the relationship between the ratios of Hg:OC and OC:N to explore the effect of litterfall decomposition on soil Hg concentrations, as suggested

TABLE 4. Soil Hg pools and residence time (RT) in the five subregions.

| | Hg pools ($mg/m^2$) | | | | | | | RT for soil horizons (yr) | |
|---|---|---|---|---|---|---|---|---|---|
| Subregion | Oie | Oa | $B_{S1}$ | $B_{S2}$ | $B_{S3}$ | Organic | Total | Organic | Total |
| ADR | 1.38 | 3.21 | 6.69 | 7.30 | 3.76 | 4.59 | 22.34 | 190 | 1820 |
| CATPOC | 1.83 | 2.94 | 5.91 | 5.66 | 2.87 | 4.77 | 19.21 | 160 | 1390 |
| CNE | 1.33 | 2.14 | 5.37 | 7.73 | 5.17 | 3.47 | 21.74 | 110 | 1950 |
| Maine | 1.31 | 1.36 | 6.52 | 6.56 | 6.25 | 2.67 | 22.00 | 100 | 1950 |
| SNE | 1.87 | 1.32 | 1.83 | 3.49 | 1.11 | 3.19 | 9.62 | 90 | 780 |
| Average | 1.46 | 2.41 | 6.12 | 6.81 | 4.51 | 3.88 | 21.32 | 140 | 2000 |

*Notes:* The average residence times were calculated excluding SNE subregion. Subregion abbreviations defined in Table 1.
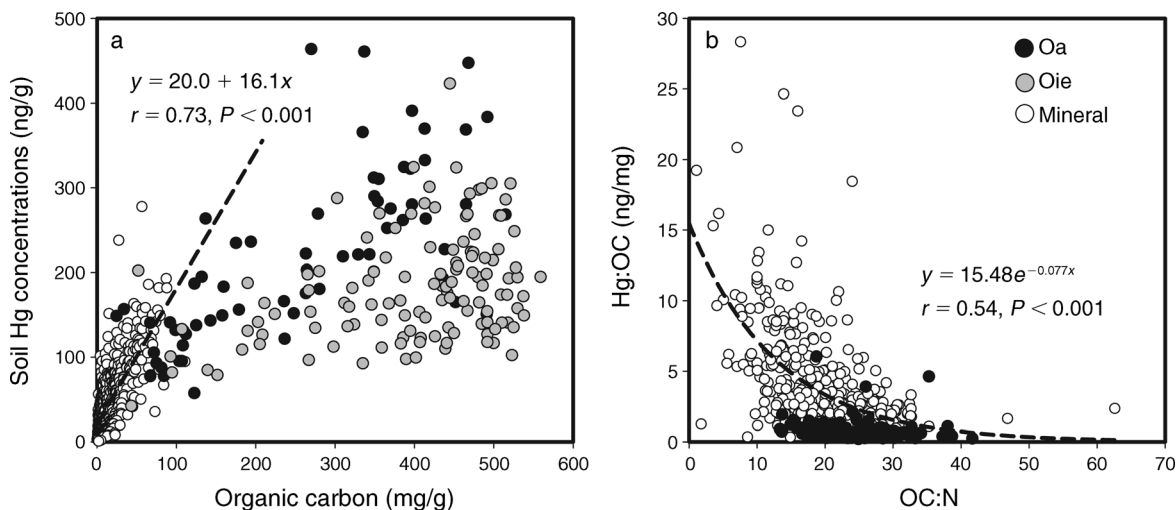
FIG. 4. (a) Relationships of Hg concentrations and organic carbon (OC) concentrations in soil profile, with short dashed line representing the relationship in the mineral horizons. (b) Relationship of Hg:OC and OC:N mass ratios in soil profile (dashed line represents relationship in all horizons). Oa is highly decomposed horizons; Oie is slightly decomposed (Oi) and moderately decomposed (Oe) grouped as a single horizon.

by Obrist et al. (2011). The ratios of Hg:OC were greater in the mineral horizons than in the organic horizons. We observed that the Hg:OC ratio decreased with increasing ratios of OC:N and increased with increasing soil depth (Fig. 4b).

Mercury concentrations in surface organic horizons increased with site elevation ($r = 0.37$, $P = 0.002$) and longitude ($r = 0.32$, $P = 0.0005$). However, we did not find a significant relationship between soil Hg concentrations or pools and current net atmospheric Hg deposition.

## Discussion

### Factors influencing spatial patterns of Hg

The results from our spatial model of net atmospheric Hg deposition are comparable to other efforts, with atmospheric Hg deposition ranging from $-3.7$–$78.1$ $\mu g \cdot m^{-2} \cdot yr^{-1}$ and inputs largely occurring as dry Hg deposition (Miller et al. 2005, 4–32 $\mu g \cdot m^{-2} \cdot yr^{-1}$; CMAQ 2005, 6.7–51.7 $\mu g \cdot m^{-2} \cdot yr^{-1}$). Higher atmospheric Hg deposition and soil Hg concentrations and pools were found in the ADR and the CATPOC regions. These two subregions likely receive higher atmospheric Hg deposition due to their closer proximity to elevated Hg emission sources in the Midwest and urban centers of the Northeast (Choi et al. 2008, Schmeltz et al. 2011) and their relatively higher elevations (Yu et al. 2011). The lack of significant correlations between current atmospheric Hg deposition and soil Hg concentrations and pools has been reported in previous investigations (Obrist et al. 2011). This relationship may be obscured by the accumulation of historically deposited Hg stored as legacy Hg in soils, historical soil formation and disturbance, and the dynamics of SOM (resulting from various forms of organic matter which effectively bind

Hg), which could influence the transfer and transformations of Hg within soil profiles in different subregions.

The close relationship between Hg and SOM concentrations in this study is consistent with observations that ionic Hg is largely complexed to functional groups of SOM, especially those containing reduced sulfur, in the organic horizon (Khwaja et al. 2006). The decomposition of SOM is linked to the transformations of Hg and hence the mass transfer of Hg (Demers et al. 2007), which likely affects the redistribution of Hg within soil profiles. With the exception of SNE, Hg concentrations, particularly pools, were generally higher in the Oa horizon than in the less decomposed Oie horizon, which might be explained by the accumulation of Hg in more stable humic substances in the Oa horizon. This horizonal pattern is also consistent with soil Hg reduction and evasion largely occurring from the Oie horizon and the immobilization of throughfall/wet Hg deposition by the Oa horizon (Demers et al. 2007, Smith-Downey et al. 2010). We observed a pattern of increasing Hg:OC ratio with increasing soil depth. Two mechanisms might help to explain these higher Hg:OC ratios in mineral soils: (1) the microbial processing of organically bound Hg to volatile $Hg^0$ is less than the overall rate of SOM decomposition on a relative basis (Obrist et al. 2011), and/or (2) some of the Hg in mineral horizons is bound to mineral surfaces, thus enhancing Hg retention despite SOM decomposition. We also observed a negative relationship between the ratios of Hg:OC and OC:N with increasing soil depth. The OC:N ratio likely reflects the magnitude of decomposition of SOM, with lower ratios representing higher degrees of decomposition. Thus, it appears that higher Hg:OC ratios in mineral soils are related to greater humification of SOM in deeper horizons.

Note that the pools of Hg in the mineral soil are greater in the northern subregions (ADR, CNE, Maine) than the subregions at lower latitudes (CATPOC, SNE). This pattern might reflect climate-induced variability in soil development. Colder conditions of the northern subregions likely limit decomposition of SOM resulting in larger pools of mineral SOM which facilitates soil accumulation of Hg.

### Pools and turnover

The concentrations of soil Hg and the estimated concentrations of background Hg in this study were in the lower range of values reported in soils of the region and worldwide (Biester et al. [2002], background Hg concentration 75 ± 25 ng/g, Europe; Zhang et al. [2006], mean 278 ng/g, range 10–966 ng/g, topsoil of Beijing, China; Demers et al. [2007], Oi horizon 305.2 ng/g, Oe horizon 394.6 ng/g, for soils in the Adirondack Park; Obrist et al. [2009], Oi 21.6 ± 1.0 ng/g, Oe 47.7 ± 3.5 ng/g, Oa 133.7 ± 6.5 ng/g, mineral horizon 7.5–35.3 ng/g, for forest soils in four Sierra Nevada forest sites, United States; Obrist et al. [2011], Oi 22–83 ng/g, Oe 48–195 ng/g, Oa 162–420 ng/g, soil 0–20 cm 11–251 ng/g, soil 40 cm 24–133 ng/g, for soils across 14 U.S. forests; Tipping et al. [2011a], average 95 ng/g for 89 UK rural topsoils). The calculated soil Hg pools are similar to values reported by Tipping et al. (2011b) for rural topsoils in the United Kingdom, Demers et al. (2007) for forest soils in the Adirondacks, and Obrist et al. (2009, 2012) for soils in a Sierra Nevada forest. The fractions of Hg stored in the organic horizons (20%) were similar to a study in the Great Lakes states (Nater and Grigal 1992).

Our data indicate that soil Hg is largely stored in the mineral horizons, although substantial pools of Hg are evident in the forest floor (12–33% of total for subregion means; Table 4). Spatially, the total soil Hg pool was the lowest in the SNE subregion, which may be due to higher $Hg^0$ evasion rates associated with higher temperature and a lower percentage of forest coverage and greater mineralization of SOM due to milder climate. The other four subregions have similar total Hg pools, but the fraction of the pool in the organic horizons was the lowest in Maine (12%).

The average total Hg deposition from 1850 to present was estimated to be 3.97 mg/m², which accounts for 102% of the current Hg pool in the organic horizon (3.88 mg/m²) and 19% of the total pool for the subregions (21.32 mg/m²) except the SNE. Subtracting the background Hg deposition (the rate prior to 1850 9.35 $\mu g \cdot m^{-2} \cdot yr^{-1}$), the average total deposition since 1850 due to anthropogenic Hg emissions is 2.49 mg/m², which is 12% of the current total soil Hg pool. This value of the contribution of anthropogenic Hg emissions to the soil pool is smaller than a global model estimate of 20% (Smith-Downey et al. 2010, Amos et al. 2013). However, our estimation of 12% contribution of current soil Hg pool from anthropogenic Hg emissions is likely underestimated due to the overestimation of background Hg deposition rate. Given current inputs and soil pools, and assuming steady-state conditions, the mean residence time for Hg in the organic horizon and the total pool is 140 years and 1800 years, respectively, in the subregions of the northeastern United States except for SNE. Soils in SNE are shallower than observed for the other subregions and have lower total Hg pools. As a result, the estimated mean residence time of Hg in the whole soil profile in SNE is considerably shorter in both the organic and mineral horizons (90 and 800 years, respectively). Our results suggest that anthropogenic activities have exacerbated Hg contamination, particularly in the forest floor, since the onset of industrialization. While soils are clearly not at steady state, these calculations are instructive to illustrate the long-term impact of atmospheric Hg deposition on soil.

There were a number of approximations that went into our analysis due to the methods used, such as the estimates of current Hg deposition and the reconstruction of historical Hg deposition. The current atmospheric Hg deposition of oxidized Hg extracted from CMAQ is likely to be overestimated due to uncertainties in the emissions inventory (annual average biases >250%, Holloway et al. 2012). The Hg emission patterns adopted from several studies and the assumptions regarding pre-1850 Hg deposition and recent declines we used are likely to contribute uncertainties to the reconstructed historical Hg deposition pattern. Note with substantial anthropogenic emissions and deposition dating back 500 years, our calculations of the total anthropogenic contributions to soils are likely underestimated. If we assume uncertainty in current atmospheric Hg deposition estimates is ±10% and the background Hg concentration is 30 ng/g, the uncertainty of our residence time calculations range from 1600 to 2000 years for the northeastern subregions other than SNE and range from 700 to 900 for SNE.

The estimated time needed to accumulate the current total pool of Hg solely by atmospheric Hg deposition is well within the time of soil formation in the glaciated landscapes of the northeastern United States (12–18k years; Ciolkosz et al. 1989). Although we did not observe a noticeable relationship between current Hg deposition and concentrations or pools of soil Hg, we did find a correlation between the total atmospheric Hg deposition since 1850 and Hg pool in the organic horizons (Fig. 5a). This pattern suggests that a major source of Hg to the forest floor is from historical atmospheric deposition. Note the relationship between total atmospheric Hg deposition since 1850 and soil Hg is considerably stronger for the Oa than the Oie horizon. We hypothesize that Oie Hg is largely derived from litter Hg inputs. Litter Hg is largely supplied from atmospheric $Hg^0$, which exhibits relatively uniform concentrations across the northern hemisphere (Mao et al. 2011, Risch et al. 2011). In contrast, Oa Hg is a combination of $Hg^0$ derived from litterfall and ionic Hg from wet and dry deposition. Deposition of ionic Hg
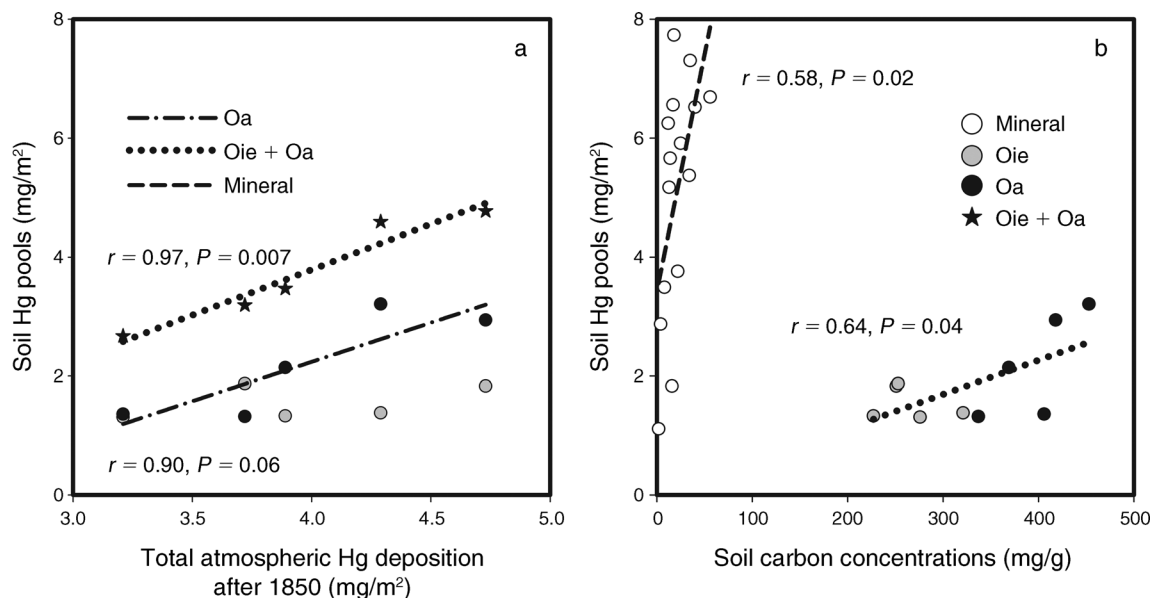
FIG. 5. (a) Relationship between estimated historical Hg deposition and pools of Hg in organic horizons. (b) Relationships of soil Hg pools with organic carbon (OC) concentrations in the organic and mineral horizons. Abbreviations defined in Fig. 4.

shows a stronger pattern of decreasing deposition than litter Hg inputs with decreases in longitude, which is consistent with the marked decrease in Oa Hg pool across the region.

The accumulation of soil Hg is linked to the formation of soils, especially to the biogeochemical dynamics of SOM. The fate of adsorbed Hg is significantly affected by the fate of the SOM. Smith-Downey et al. (2010) suggested that the supply of binding sites associated with SOM is not a limiting factor (maximum storage capacity 0.024 g Hg/g C) for the accumulation of Hg in soils (Hintelmann et al. 2002). The pool of Hg is correlated with soil OC content in both the organic and mineral horizons (Fig. 5b). The turnover time of soil OC varies from several months in the Oie horizon, to a few years in the Oa horizon, and to thousands of years in the mineral horizons (Schimel et al. 1994, Zhang et al. 2010). Therefore, Hg adsorbed to relatively short-lived labile OC in the forest floor is either reduced to $Hg^0$ and subject to evasion, transported hydrologically, or accumulated in more stable SOM in lower soil horizons. Mercury that binds to recalcitrant OC in the mineral horizons is more resistant to transformation, leading to long-term accumulation and higher Hg:OC ratios in mineral horizons. Increases in Hg:OC may also be linked to increased availability of N that facilitates decomposition of OC. The considerable discrepancy between the current total pools of soil Hg and the possible atmospheric Hg inputs over the period of soil formation (e.g., for 15k years, 140 mg/m$^2$) might be explained by the different immobilization capacities of soil at different stages of formation. A large fraction of deposited Hg is currently evaded back to the atmosphere (Denkenberger et al. 2011). Conditions that affect the dynamics of SOM, which include climate, land-use change, and landscape disturbance therefore are likely, to a large extent, drive the spatial patterns of concentrations and pools of soil Hg.

## CONCLUSIONS

Our spatial model showed higher atmospheric Hg deposition in the CATPOC and ADR subregions due to their higher elevation and closer proximity to the elevated Hg emission source area of the Midwest and urban areas of the Mid-Atlantic and southern New England. Dry Hg deposition exceeded wet Hg deposition. Soils in the northeastern United States were a net sink for atmospheric Hg.

We did not observe any significant correlations between concentrations or pools of soil Hg and current net atmospheric Hg deposition. However, a relationship was evident between the cumulative atmospheric Hg deposition after 1850 and Hg pools in the organic horizons, with higher correlation in the Oa horizon.

Soil Hg concentrations were significantly correlated with SOM, with a stronger relationship in the mineral horizons. Soil OC concentrations were correlated with soil Hg pools in the mineral horizons and Oa horizon, but not in the Oie horizon. While atmospheric Hg deposition contributes to the accumulation of soil Hg, the dynamics of SOM (e.g., OC and N) shapes the horizontal distribution of Hg in the northeastern U.S. soils.

LITERATURE CITED

Amos, H. M., D. J. Jacob, D. G. Streets, and E. M. Sunderland. 2013. Legacy impacts of all-time anthropogenic emissions on the global mercury cycle. Global Biogeochemical Cycles 27:410–421.

Arnold, R. W., and H. Eswaran. 1993. Soil horizon use by the U.S. Soil Survey. Catena 20:375–381.

Biester, H., R. Bindler, A. Martinez-Cortizas, and D. R. Engstrom. 2007. Modeling the past atmospheric deposition of mercury using natural archives. Environmental Science and Technology 41:4851–4860.

Biester, H., G. Muller, and H. F. Scholer. 2002. Estimating distribution and retention of mercury in three different soils contaminated by emissions from chlor-alkali plants: part I. Science of the Total Environment 284:177–189.

Bookman, R., C. Driscoll, D. R. Engstrom, and S. W. Effler. 2008. Local to regional emission sources affecting mercury fluxes to New York lakes. Atmospheric Environment 42:6088–6097.

Choi, H. D., T. M. Holsen, and P. Hopke. 2008. Atmospheric mercury (Hg) in the Adirondacks: concentrations and sources. Environmental Science and Technology 42:5644–5653.

Church, M. R., et al. 1989. Future effects of long-term sulfur deposition on surface water chemistry in the northeast and southern Blue Ridge Province. Technical Report EPA/600/3-89/061a. U.S. Environmental Protection Agency, Washington, D.C., USA.

Ciolkosz, E. J., W. J. Waltman, T. W. Simpson, and R. R. Dobos. 1989. Distribution and genesis of soils of the northeastern United States. Geomorphology 2:285–302.

CMAQ. 2005. Deposition mapping. Community Multiscale Air Quality Program, U.S. EPA, Washington, D.C. http://epa.gov/AMD/Data/wdtData.html

Daly, C., G. H. Taylor, and W. P. Gibson. 1997. The PRISM approach to mapping precipitation and temperature. Pages 10–12 in Proceedings of the 10th AMS Conference on Applied Climatology, Reno, Nevada, October 20–23, 1997. American Meteorological Society, Boston, Massachusetts, USA.

De Vos, B., M. V. Meirvenne, P. Quataert, J. Deckeres, and B. Muys. 2005. Predictive quality of pedotransfer functions for estimating bulk density of forest soils. Soil Science Society of America Journal 69:500–510.

Demers, J. D., C. T. Driscoll, T. J. Fahey, and J. B. Yavitt. 2007. Mercury cycling in litter and soil in different forest types in the Adirondack region, New York, USA. Ecological Applications 17:1341–1351.

Denkenberger, J. S., C. T. Driscoll, B. A. Branfireun, C. S. Eckley, M. Cohen, and P. Selvendiran. 2011. A synthesis of rates and controls on elemental mercury evasion in the Great Lakes Basin. Environmental Pollution 161:291–298.

Dittman, J. A., J. B. Shanley, C. T. Driscoll, G. R. Aiken, A. T. Chalmers, J. E. Towse, and P. Selvendiran. 2010. Mercury dynamics in relation to dissolved organic carbon concentration and quality during high flow events in three northeastern U.S. streams. Water Resource Research 46:w07522.

Drevnick, P., et al. 2011. Spatial and temporal patterns of mercury accumulation in lacustrine sediments across the Laurentian Great Lakes region. Environmental Pollution 161:252–260.

Driscoll, C. T., Y. J. Han, C. Y. Chen, D. C. Evers, K. F. Lambert, T. M. Holsen, N. C. Kamman, and R. K. Munson. 2007. Mercury contamination in forest and freshwater ecosystems in the Northeastern United States. BioScience 57:17–28.

Driscoll, C. T., R. P. Mason, H. M. Chan, D. J. Jacob, and N. Pirrone. 2013. Mercury as a global pollutant: sources, pathways, and effects. Environmental Science and Technology 47:4967–4983.

Driscoll, C. T., et al. 2003. Nitrogen pollution in the Northeastern United States: sources, effects and management options. BioScience 53:357–374.

Engstrom, D. R., and E. B. Swain. 1997. Recent declines in atmospheric mercury deposition in the upper Midwest. Environmental Science and Technology 312:960–967.

Evers, D. C., et al. 2008. Adverse effects from environmental mercury loads on breeding common loons. Ecotoxicology 17:69–81.

Evers, D. C., Y. J. Han, C. T. Driscoll, N. C. Kamman, M. W. Goodale, K. F. Lambert, T. M. Holsen, C. Y. Chen, T. A. Clair, and T. Butler. 2007. Biological mercury hotspots in the Northeastern United States and Southeastern Canada. BioScience 57:29–43.

Evers, D. C., A. K. Jackson, T. H. Tear, and C. E. Osborne. 2012. Hidden risk: mercury in terrestrial ecosystems of the Northeast. Technical Report: 2012-07. Biodiversity Research Institute, Gorham, Maine, USA.

Federer, C. A., D. E. Turcotte, and C. T. Smith. 1992. The organic fraction–bulk density relationship and the expression of nutrient content in forest soils. Canadian Journal of Forest Research 23:1026–1032.

Fitzgerald, W. F., D. R. Engstrom, R. P. Mason, and E. A. Nater. 1998. The case for atmospheric mercury contamination in remote areas. Environmental Science and Technology 32:1–7.

Golden, M. L. 2010. Keys to soil taxonomy. 11th edition. USDA, Soil Survey Division, Natural Resources Conservation, Washington, D.C., USA.

Grigal, D. F. 2002. Inputs and outputs of mercury from terrestrial watersheds: a review. Environmental Review 10:1–39.

Hintelmann, H., R. Harris, A. Heyes, J. P. Hurley, C. A. Kelly, D. P. Krabbenhoft, S. Lindberg, J. W. M. Rudd, K. J. Scott, and V. L. St. Louis. 2002. Reactivity and mobility of new and old mercury deposition in a boreal forest ecosystem during the first year of the METAALICUS study. Environmental Science and Technology 36:5034–5040.

Hissler, C., and J. L. Probst. 2006. Impact of mercury atmospheric deposition on soils and streams in a mountainous catchments (Vosges, France), polluted by chlor-alkali industrial activity: the important trapping role of the organic matter. Science of the Total Environment 361:153–178.

Holloway, T., C. Voigt, J. Morton, S. N. Spak, A. P. Rutter, and J. J. Schauer. 2012. An assessment of atmospheric mercury in the Community Multiscale Air Quality (CMAQ) model at an urban site and a rural site in the Great Lakes Region of North America. Atmospheric Chemistry and Physics 12:7117–7133.

Howard, P. J. A., and D. M. Howard. 1989. Use of organic carbon and loss-on-ignition to estimate soil organic matter in different soil types and horizons. Biology and Fertility of Soils 9:306–310.

Huntington, T. G., C. E. Johnson, A. H. Johnson, T. G. Siccama, and D. F. Ryan. 1989. Carbon, organic matter, and bulk density relationships in a forested spodosal. Soil Science Society of America Journal 148:380–386.

Hurley, J. P., J. M. Benoit, C. L. Babiarz, M. M. Shafer, A. W. Ander, J. R. Sullivan, R. Hammond, and D. A. Webb. 1995. Influences of watershed characteristics on mercury levels in Wisconsin Rivers. Environmental Science and Technology 29:1867–1875.

Khwaja, A. R., P. R. Bloom, and P. L. Brezonik. 2006. Binding constants of divalent mercury ($Hg^{2+}$) in soil humic acids and soil organic matter. Environmental Science and Technology 40:844–849.

Lee, J., R. Church, D. Lammers, L. Liegel, M. Johnson, D. Coffey, R. Holdren, D. Stevens, R. Turner, and L. Blume. 1989. Watershed surveys to support an assessment of the

regional effects of acidic deposition on surface water chemistry. Journal of Environmental Management 13:273–294.

Lorey, P., and C. T. Driscoll. 1999. Historical trends of mercury deposition in Adirondack lakes. Environmental Science and Technology 33:718–722.

Mao, H., R. Talbot, J. Hega, and J. Koermer. 2011. Speciated mercury at marine, coastal, and inland sites in New England—part 2: relationships with atmospheric physical parameters. Atmospheric Chemistry and Physics 11:28395–28443.

Miller, E. K., A. Vanarsdale, G. J. Keeler, A. Chalmers, L. Poissant, N. C. Kamman, and R. Brulotte. 2005. Estimation and mapping of wet and dry mercury deposition across northeastern North America. Ecotoxicology 14:53–70.

NADP MDN. 2011. National Atmospheric Deposition Network, Mercury Deposition Network Data. National Atmospheric Deposition Network, Mercury Deposition Network, Champaign, Illinois, USA. http://nadp.sws.uiuc.edu/nadpdata/mdnalldata.asp

Nater, E. A., and D. Grigal. 1992. Regional trends in mercury distribution across the Great Lakes states, north central USA. Nature 358:139–141.

Obrist, D., et al. 2011. Mercury distribution across 14 U.S. forests. Part 1: spatial patterns of concentrations in biomass, litter, and soils. Environmental Science and Technology 45:3977–3981.

Obrist, D., D. W. Johnson, and R. L. Edmonds. 2012. Effects of vegetation type on mercury concentrations and pools in two adjacent coniferous and deciduous forests. Journal of Plant Nutrition and Soil Science 175:68–77.

Obrist, D., D. W. Johnson, and S. E. Lindberg. 2009. Mercury concentrations and pools in four Sierra Nevada forest sites and relationships to organic carbon and nitrogen. Biogeosciences 6:765–777.

Pirrone, N., et al. 2010. Global mercury emission to the atmosphere from anthropogenic and natural sources. Atmospheric Chemistry and Physics 10:5951–5964.

Rimmer, C. C., E. K. Miller, K. P. McFarland, R. J. Taylor, and S. D. Faccio. 2010. Mercury bioaccumulation and trophic transfer in the terrestrial food web of a montane forest. Ecotoxicology 19:697–709.

Risch, M. R., J. DeWild, D. P. Krabbenhoft, R. K. Kolka, and L. Zhang. 2011. Litterfall mercury dry deposition in the eastern USA. Environmental Pollution 161:284–290.

Schimel, D. S., B. H. Braswell, E. A. Holland, R. McKeown, D. S. Ojima, T. H. Painter, W. J. Parton, and A. R. Townsend. 1994. Climatic, edaphic and biotic controls over storage and turnover of carbon in soils. Global Biogeochemical Cycles 8:279–294.

Schmeltz, D., et al. 2011. MercNet: a national monitoring network to assess responses to changing mercury emissions in the United States. Ecotoxicology 20:1713–1725.

Schuster, P. F., D. P. Krabbenhoft, D. L. Naftz, D. Cecil, M. L. Olson, J. F. Dewild, D. D. Susong, J. R. Green, and M. L. Abbott. 2002. Atmospheric mercury deposition during the last 270 years: a glacial ice core record of natural and anthropogenic sources. Environmental Science and Technology 36:2303–2310.

Selvendiran, P., C. T. Driscoll, J. T. Bushey, and M. R. Montesdeoca. 2008. Wetland influence on mercury fate and transport in a temperate forested watershed. Environmental Pollution 154:46–55.

Smith-Downey, N. V., E. M. Sunderland, and D. J. Jacob. 2010. Anthropogenic impacts on global storage and emissions of mercury from terrestrial soils: insights from a new global model. Journal of Geophysical Research 115:G03008.

St. Louis, V., J. W. M. Rudd, C. A. Kelly, B. D. Hall, K. R. Rolfhus, K. J. Scott, S. E. Lindberg, and W. Dong. 2001. Importance of the forest canopy to fluxes of methyl mercury and total mercury to boreal ecosystems. Environmental Science and Technology 35:3089–3098.

Streets, D. G., M. K. Devane, Z. Lu, T. C. Bond, E. M. Sunderland, and D. J. Jacob. 2011. All-time releases of mercury to the atmosphere from human activities. Environmental Science and Technology 45:10485–10491.

Swain, E. B., D. R. Engstrom, M. E. Brigham, T. A. Henning, and P. L. Brezonik. 1992. Increasing rates of atmospheric mercury deposition in midcontinental North America. Science 257:784–787.

Tipping, E., J. M. Poskitt, A. J. Lawlor, R. A. Wadsworth, D. A. Norris, and J. R. Hall. 2011a. Mercury in United Kingdom topsoils: concentrations, pools, and critical limit exceedances. Environmental Pollution 159:3721–3729.

Tipping, E., R. A. Wadsworth, D. A. Norris, J. R. Hall, and I. Ilyin. 2011b. Long-term mercury dynamics in UK soils. Environmental Pollution 159:3474–3483.

Townsend, J., and C. T. Driscoll. 2013. Red-backed salamander (Plethodon cinereus) as a bioindicator of mercury in terrestrial forests of the northeastern United States. Ecological Indicators 34:168–171.

U.S. Geological Survey. 2011. Forest cover types. National Geospatial Program, United States Geological Survey, Reston, Virginia, USA. http://nationalatlas.gov/maplayers.html?openChapters=chpbio#chpbio

Warby, R. A. F., C. E. Johnson, and C. T. Driscoll. 2005. Chemical recovery of surface waters across the northeastern United States from reduced inputs of acidic deposition: 1984–2001. Environmental Science and Technology 39:6548–6554.

Warby, R. A. F., C. E. Johnson, and C. T. Driscoll. 2009. Continuing acidification of organic soils across the Northeastern USA: 1984–2011. Soil Science Society of America Journal 73:274–284.

Yu, X., C. T. Driscoll, J. Huang, T. Holsen, and B. Blackwell. 2013. Modeling and mapping of atmospheric mercury deposition in Adirondack Park, New York. PLoS ONE 8(3):e59322.

Yu, X., C. T. Driscoll, M. Montesdeoca, D. Evers, M. Duron, K. Williams, N. Schoch, and N. C. Kamman. 2011. Spatial patterns of mercury in biota of Adirondack, New York lakes. Ecotoxicology 20:1543–1554.

Zhang, L., Y. Luo, G. Yu, and L. Zhang. 2010. Estimating carbon residence times in three forest ecosystems of eastern China: applications of probabilistic inversion. Journal of Geophysical Research 115:G01010.

Zhang, X., K. Luo, X. Sun, J. Tan, and Y. Lu. 2006. Mercury in the topsoil and dust of Beijing City. Science of the Total Environment 368:713–722.

SUPPLEMENTAL MATERIAL

### Appendix

Texts summarizing the quality control and quality assurance (QA/QC) procedures and the method of estimating atmospheric Hg deposition (*Ecological Archives* A024-047-A1).

# ERRATA

Melvin et al., wish to report an error in their paper "Forest liming increases forest floor carbon and nitrogen stocks in a mixed hardwood forest" published in December 2013 *Ecological Applications* 23:1962–1975, that was caused by a misinterpretation of inorganic nitrogen units reported from auto analyzer output (values were in units of mg nitrogen, but had been interpreted as mg of either ammonium or nitrate). Correcting and re-analyzing the data does not change the main findings of the paper, but it does influence the results presented in one figure (Fig. 4). All y-axis values increase as a result of the systematic correction factor that had been applied to the data for either ammonium or nitrate. Patterns and statistical relationships do not change, with the exception of panel (A) in the figure, which no longer shows a significant difference between treatments. The corrected figure is presented here.
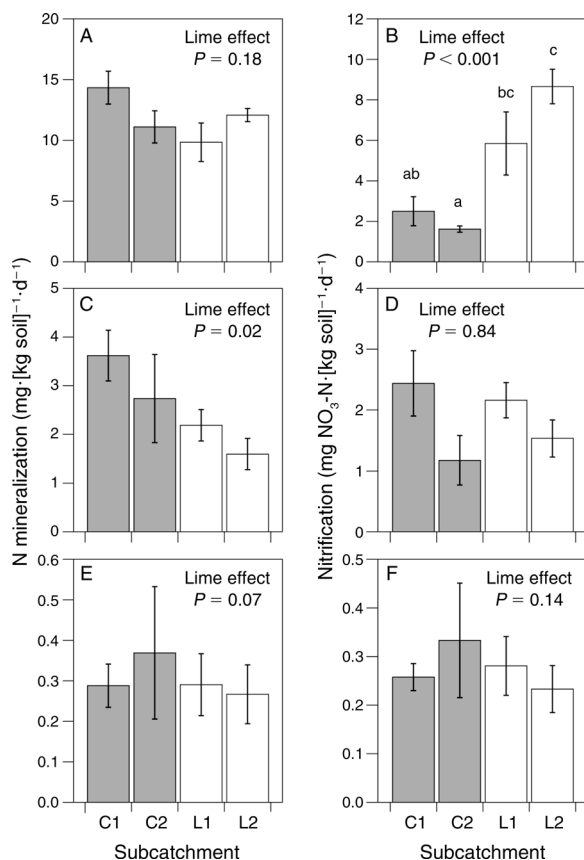


Xue Yu reported an error in Eq. 2 of the Hu et al. paper published in the June 2014 issue (Xue Hu, Charles T. Driscoll, Richard A. F. Warby, Mario Montesdeoca, and Chris E. Johnson. 2014. Soil mercury and its response to atmospheric mercury deposition across the northeastern United States. *Ecological Applications* 24:812–822). The correct equation should read:

$$\ln(B_i) = 0.263 - 0.147\ln(OC‰)_i - 0.103\ln^2(OC‰)_i \tag{2}$$

without the subscript 2 at the end of the published equation.

This typo in the final paper apparently stemmed from an error made in the editorial office when the proofs were being corrected for publication of the issue. We apologize to the authors and our readers.